Full Paper

MICROSTRUCTURAL RESPONSE OF POWDER METALLURGY (PM) RR1000 SUPERALLOY TO INERTIA FRICTION WELDING

K.M. Oluwasegun
Department of Materials Science and Engineering, Obafemi Awolowo University, Ile-Ife, Osun State 220005 Nigeria.

M.O. Adeoye
Department of Materials Science and Engineering, Obafemi Awolowo University, Ile-Ife, Osun State 220005 Nigeria
madeoye@oauife.edu.ng

O.E. Olorunniwo,
Department of Materials Science and Engineering, Obafemi Awolowo University, Ile-Ife, Osun State 220005 Nigeria.

P.O. Atanda
Department of Materials Science and Engineering, Obafemi Awolowo University, Ile-Ife, Osun State 220005 Nigeria.

ABSTRACT

The microstructural response of powder metallurgy RR1000 superalloy to inertia friction welding was investigated. It was observed that the rapid heating during inertial friction welding resulted in a significant grain-boundary liquation of solid-state γ' precipitates, low temperature melting depressant intermetallic compound, and secondary solidification MC carbides constituents, which were all present in the preweld heat-treated alloy. Liquation of these particles enhanced grain boundary microfissuring in the thermomechanical affected zone (TMAZ) of the weldment. However, contrary to the generally observed increase in HAZ cracking in superalloys with an increase in Ti and Al concentration, due to increase in the hardness of the alloy and rapid re-precipitation of γ' strengthening particles during cooling from welding temperature, a significantly reduced cracking was observed in inertia friction welded PM RR1000 compared to the conventional gas tungsten arc welded cast IN738. This was despite the hardness being higher in the former than in the latter. This may be related to the solid state welding phenomena proffered by inertia friction welding which precludes the formation of liquid melt during welding.

Keywords: *Hardness; Intermetallic compounds; Superalloy; Grain boundary wetting*

1. INTRODUCTION

RR1000 is an emerging precipitation-strengthened nickel based superalloy produced via powder metallurgy. This alloy possesses a very good hot-corrosion resistance, long-term stability, and high-temperature strength, primarily due to the precipitation hardening by γ' precipitates, an ordered intermetallic $Ni_3(Al,Ti)$ phase dispersed in the austenitic γ' matrix, and has been employed for use in aero-engines and large stationary power generation gas turbine discs. Powder metallurgy processing of the alloy results in a further improvement in its high-temperature properties and hot corrosion resistance and also permits the use of higher service temperatures, which is very important for enhancing the thermal efficiency of turbines (Silva and Brito, 2006). The hot-section components of the turbines generally experience very severe thermal and mechanical stresses for extended periods during service, which can cause cracking or material loss. For cost effectiveness, it is often advantageous to repair the damaged components rather than replace them, and inertia friction welding has been found as a better joining technique than the conventional welding method during repair to increase the component life. However, precipitation-strengthened nickel-base alloys that contain a high concentration of Al/Ti (›3 at%) exhibit only a limited weldability due to their high susceptibility to heat-affected zone (HAZ) cracking during welding and during the subsequent postweld heat treatment (PWHT) (Owezarski et al, 1966; Prager and Sines, 1970; Jahnke, 1982; Thamburaj et al, 1983; Ojo et al, 2004; Sidhu et al, 2005).

Cracking during welding of nickel base superalloy has been attributed mostly to shrinkage stresses caused by rapid re-precipitation of γ' particles during weld cooling and the propensity of the alloys to liquation cracking due to constitutional liquation of various phases present in the preweld microstructure of the base alloy (Owezarski et al, 1966) . Strain-age or PWHT cracking in all the precipitation-hardened superalloys, has also been reported to generally initiate in the HAZ that liquated during the welding process (Lim et al, 2002; Sidhu et al, 2005). The synergetic effect of thermally induced welding strain and very low ductility in the alloy due to localized melting of particle at grain boundaries results in HAZ liquation cracking. HAZ or thermomechanical affected zone (TMAZ) liquation is known to occur either by non-equilibrium interface melting below the solidus an alloy or by equilibrium supersolidus melting. Subsolidus HAZ liquation which commonly occurs by constitutional liquation of second phase particles is generally considered more detrimental to crack resistance in that it extends the effective melting range of an alloy and also influences the nature of supersolidus melting by pre-establishing non-equilibrium film at a lower temperature which changes the reaction kinetics during subsequent heating (Owezarski et al, 1966). This process, proposed by Pepe and Savage (Pepe and Savage, 1967) and observed by different investigators in various alloy system (Romig et al, 1988; Radhakrishnan and Thompson, 1991; Reiso et al, 1993), occurs by a eutectic-type reaction between a second phase particle and the matrix producing a non-equilibrium solute rich film at the particle/matrix interface. Thus the thermal history is particularly important if weld microstructures are to be optimized for subsequent joint performace. The present study is aimed at microstructural response of the newly developed PM RR1000 superalloy to inertia friction welding.

2. EXPERIMENTAL PROCEDURE

The base alloy in this work was a new generation PM nickel base superalloy RR1000, developed and provided by Rolls Royce Plc. The as received base alloy had been standard solution heat treated at 1120°C for 4 h and fully aged at 760°C for 8 h with subsequent air cooling after the PM process with the following composition (wt %) 15Cr, 16.5Co, 5Mo, 3Al, 3.9Ti, 2Ta, 0.2Hf, 0.02B, 0.05Zr, 0.02C and nickel balance. The as received inertial friction welded (IFW) samples were of dimensions 20 mm × 12 mm × 10 mm. The themomechanical affected zone microstructures of this alloy were simulated by a Gleeble thermomechanical simulation system by using cylindrical specimens of 8 mm diameter and 7.96 mm length which were heated to 1150, 1175, 1200 and 1225°C at a rate of 20°C/s and held for 1 s at all temperatures followed by water quenching, while another similar sample was air cooled. The specimen temperature was monitored with a chromel-alumel thermocouple spot welded to the specimens at the midsection of the gauge length. The specimens were water quenched from their high temperatures in order to preserve, as much as possible, the microstructural changes that occurred at the simulation temperatures. The as received inertial friction welded samples were sectioned transversely across the weldment while the Gleeble simulated samples were sectioned at the locations of the spot welded thermocouple. The sectioned samples were polished using standard metallographic techniques and were subsequently electrolytically etched in 10% orthophosphoric acid solution at 3.5 V for 3 s. TEM foils were prepared by twin jet electropolishing in a solution containing 35 cc $HClO_4$ in 500 cc methanol and 65 cc n-butanol at 20 V and a temperature ≤ -40°C. Vickers hardness test was carried out by employing a Mitutoyo vicker harness tester with a load of 1000 g. The microstructural studies of the specimens were carried out by the use of optical microscope, field emission gun XL30 scanning electron microscope and Philips CM20 transmission electron microscope, both electron microscopes equipped with energy dispersive X-ray (EDX) spectrometer.

3. RESULTS AND DISCUSSION

3.1. Microstructure of preweld material

The microstructure of the as-received preweld (solution treated) RR1000 superalloy is shown in Fig. 1. It consisted of extensive precipitation, ~48 vol %, of trimodal ordered intermetallic phase within the grain and at the grain boundary regions. It is seen that they have a spherical morphology. They consisted of a fairly regular distribution of primary γ', 0.8–2 μm in size, fine (~0.1 μm) spheroidal secondary γ', and very fine tertiary γ' (5-30 nm) (Fig. 1(a) and (b)). Figure 1(c) shows a thin film TEM bright field image of the spheroidal secondary γ' particles. Superlattice reflections in the SADP, shown confirmed them to be ordered intermetallic γ' phase with the usual orientation relationship of $\{100\}_{\gamma'}$ //$\{100\}_{\gamma}$ and $\langle 100\rangle_{\gamma'}$//$\langle 100\rangle_{\gamma}$ with the fcc-γ matrix. These secondary γ' particles have formed during cooling from the solution treatment temperature. Metal carbides (MC) rich in Ti were also observed in the alloy (Fig. 1(a) and 2(d)).

3.2. Microstructures of the actual and simulated TMAZ

The microstructure of the actual weldment and simulated TMAZ showed similar morphology of microcracks displaying a relatively irregular and jagged path typical of liquation cracks, with cracking occurring pre-dominantly in the TMAZ slightly away from the bond line (Fig. 2). Detailed examination of cracked regions at higher magnification by SEM revealed the existence of re-solidification constituents with eutectic morphology that is characteristic of γ-γ' eutectic which formed at the later stage of solidification in this alloy (Fig. 2(f)). The re-solidification constituents that formed mostly on one side of the cracks confirm the formation of liquid film on the grain boundaries in TMAZ by liquation mechanism. Microfissuring occurred by decohesion across the solid–liquid interfaces under the action of tensile welding stresses generated during cooling.

Moreover, many of the liquated grain boundaries were observed to exhibit liquid-film migration features (Fig. 2(d)), signifying the formation of grain-boundary liquid during the weld thermal cycle. The liquid was observed to be present in the form of thick, continuous layers, particularly along the grain-boundary regions in the immediate vicinity of the fusion zone. It has been reported that grain-boundary liquation, observed in welds of many fully austenitic iron and nickel-based alloys aggravate the intergranular microfissuring in these materials, which has generally been attributed to the inability of the intergranular liquid to accommodate thermal and mechanical stresses and mechanical constraint during weld cooling (Radhakrishnan and Thompson, 1991; Nakkalil et al, 1992; Ojo et al, 2004).

3.3. Constitutional liquation of γ' precipitates and its attendant effect on grain boundary microfissuring

Constitutional liquation of γ' precipitates, which are the principal precipitation-strengthening particles in RR1000 superalloy, was observed to be a significant phenomenon that occurred in the TMAZ of the present welds. The extent of γ' liquation in the welded samples was observed to increase with an increase in the peak temperatures experienced in the TMAZ as illustrated by the simulation results (Fig. 3(a) and (b)).This was also true for the actual welded sample with proximity to the fusion line (Fig. 4). The requirement for the occurrence of constitutional liquation of an intermetallic compound A_xB_y in an alloy is the existence of A_xB_y particles at temperatures equal to or above their eutectic temperature on heating (Ojo et al, 2004). Consequently, the susceptibility of an A_xB_y type second phase to constitutional liquation in the weld TMAZ must primarily be related to its solid state dissolution behavior, as complete dissolution prior to reaching the eutectic temperature will preclude the occurrence of liquation. It has been reported that the terminal eutectic temperature in a nickel base superalloy (Inconel 718) above which constitutional liquation of A_2B-type Laves phase and NbC particles were observed was found to correspond to the terminal reaction peak temperature during thermal analysis (Radhakrishnan and Thompson, 1991). Dissolution behavior of γ' precipitates was expected to deviate from equilibrium due to rapid thermal cycling

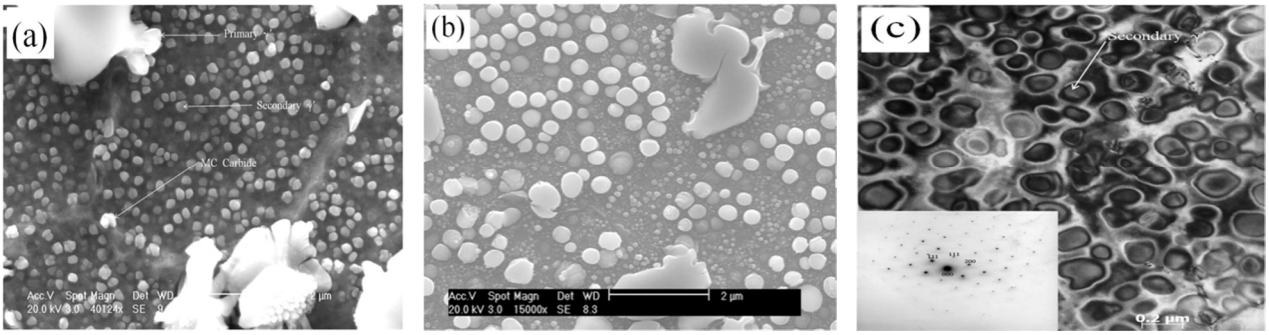

Fig. 1. (a) and (b) Micrographs showing trimodal distribution of γ' precipitate. (c) TEM bright field image showing secondary γ' particles with (inset) selected area diffraction pattern (SADP) from $[0\bar{1}1]$ *zone axis*

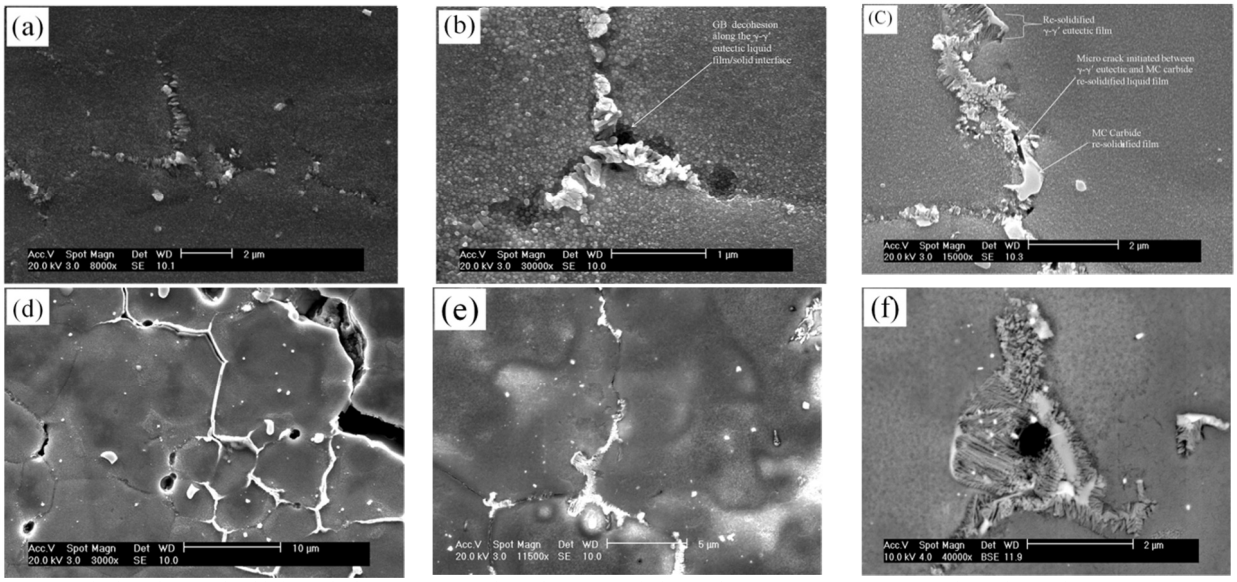

Fig. 2. SEM micrograph of (a) the actual welded sample showing microcracks at the TMAZ, (b) the simulation at 1175°C + water quench, (c) the simulation at 1200°C + water quench, (d and e) simulated TMAZ showing continuous layer of constitutional liquated particles. (f) Backscatter electron mode of SEM showing typical morphology of γ-γ' eutectic product and crack formed by decohesion of solid-liquid interface.

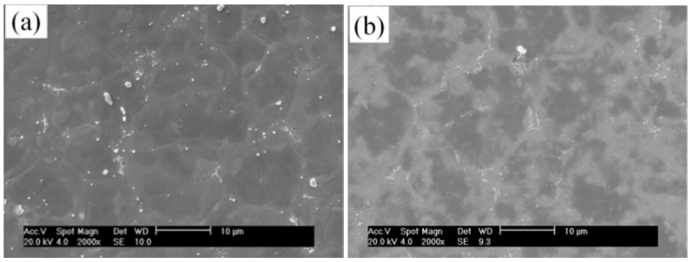

Fig. 3. SEM micrographs showing the extent of liquation at different peak simulation temperature (a) 1175°C and (b) 1200°C.

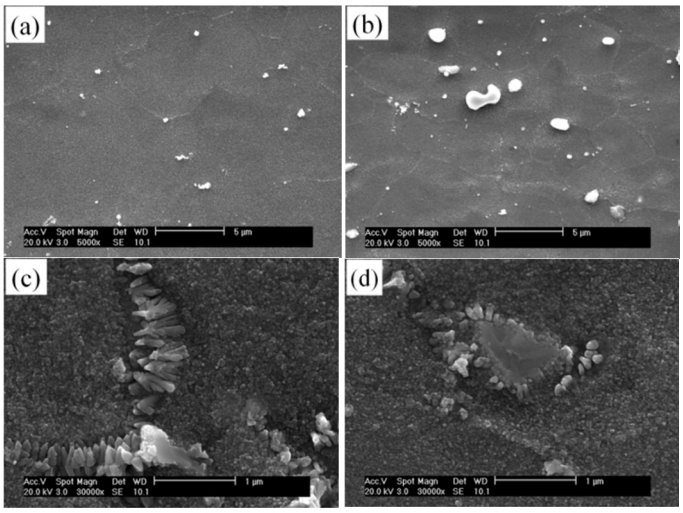

Fig.4. SEM micrographs showing the extent of γ' liquation as a function of distance from bond line (a) and (d) at 2 μm from bond line and (b) and (c) 4 μm from bond line.

involved during welding. Particle dissolution model under rapid heating condition by an analytical technique as well as through the additivity and isokinetic approach has been made (Bjorneklett et al, 1998). The results of the two methods, which were found to be in good agreement with numerical dissolution model and experimental results, show that the degree of particle dissolution depends on interplay between the heating rate and the initial particle size. The solid state dissolution of the γ' phase in Astroloy superalloy at equilibrium and under rapid heating was studied by Soucail and Bienvenu (Soucail and Bienvenu, 1996) in a separate work. Their results, which were in agreement with those of Bjorneklett et al. (1998) showed that there was a significant deviation from equilibrium under rapid heating condition, in that the temperature of complete solid state dissolution increased with increasing heating rate and this deviation was dependent on the initial particle size. This increase in complete dissolution temperature was found to be more pronounced with increase in particle size. An increase of about 120°C in complete dissolution temperature was reported for γ' precipitates with initial size of 0.8 μm under a heating rate of 8°C/s. In inertia friction welding process, like the one used in the present work, typical heating rate normally exceeds 150°C/s and as such, variations in γ' dissolution behaviour of γ' particles could be expected to depend on the particle's location and size, with the possibility of some coarse particles remaining undissolved above 1600°C (solvus temperature of primary γ') resulting in their constitutional liquation. Evidence of γ/γ' interface liquation was observed not only along the grain boundaries but more importantly within the grains of the TMAZ (Fig. 5). This figure is presented to prevent argument that liquation of intergranular γ' particles could not be used to confirm the occurrence of constitutional liquation of the precipitate, knowing that other liquation mechanisms may also be operative at grain boundaries, such as constitutional liquation of MC type carbides and possibly liquation due to segregation of low melting point depressing elements like titanium. Consequently intragranular particles shown in Fig. 5 is located up to 10 μm away from HAZ grain boundaries and distinctly separated from other liquating phases.

Susceptibility to cracking depends on penetration and wetting of grain boundary liquid film thickness and its stability to temperatures at which sufficient thermal and mechanical stresses are generated on cooling. This is very crucial because mere occurrence of liquation may not be sufficient to produce a crack susceptible microstructure. Grain boundary wetting is enhanced if the solid–liquid interfacial energy is small compared to the grain boundary energy. Considering that the metastable liquid produced by constitutional liquation always reacts with the solid through solute back diffusion, the non-equilibrium solid–liquid interface energy is very low (Askay et al, 1974), and as such extensive grain boundary penetration and wetting by film produced by constitutional liquation of γ' particles is expected. This was observed in all the samples with significant penetration and spreading of the film along the grain boundary (Figs. 2(c) to (f)), even to the lower temperature subsolidus region of the TMAZ.

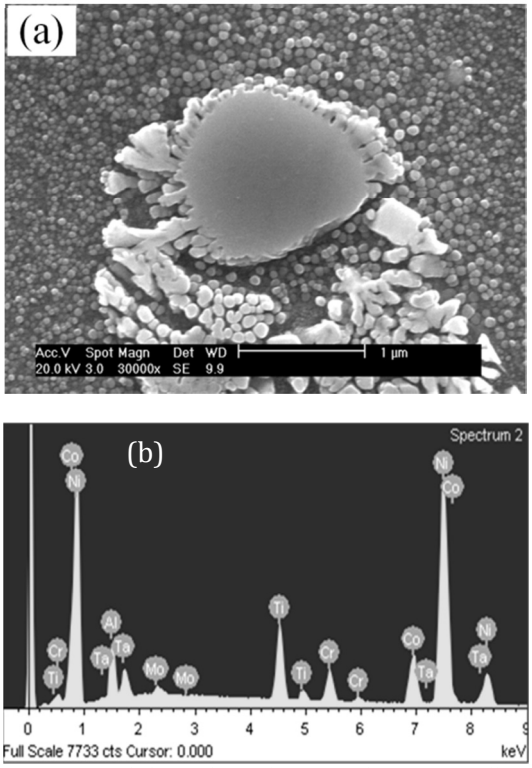

Fig. 5. (a) SEM micrograph showing liquated transgranular primary γ'. (b) EDX of liquated intragranular primary γ'.

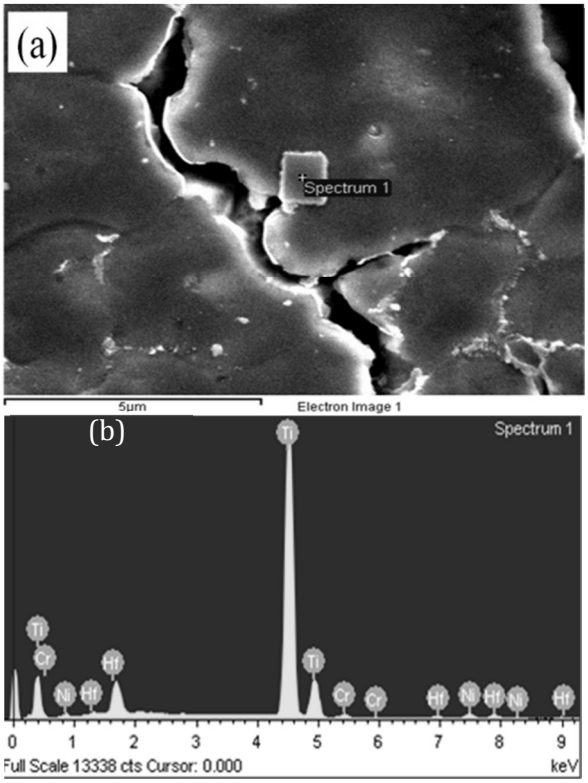

Fig.6. (a) SEM micrograph showing grain boundary Ni-Ti intermetallic particle. (b) EDX of the Ti rich precipitate.

3.4. The Role of MC and Ti-rich particles in the TMAZ microfissuring

The role of carbides in superalloys is complex and dynamic. Opinions seem to vary as to whether carbides are to be tolerated or are essential in the superalloy grain boundaries. However most investigators today feel carbides do exert a significant and beneficial effect on rupture strength at high temperature. However, our focus should not be drifted from the fact that carbide morphology can influence ductility and chemical stability of the matrix through removal of reacting elements. The solvus temperatures of MC carbides have been reported to be within the range of 1180-1190°C (Koul and Wallace,1982). The high heating rate of the weld region or of the simulated samples increases the solvus temperature of this particle as discussed in γ' liquation. The existence of these particles up to the temperature at which they can form an eutectic like reaction, MC + γ with the matrix γ resulted in constitutional liquation of Ti-rich MC to form liquid film spreading along the grain boundary (Fig. 2(d)).

The dissolution of the secondary γ' and liquation of both primary γ' and Ti- rich MC carbide in the TMAZ resulted in the microsegregation of Ti to the grain boundary due to the positive segregation behaviour proffers by its partition coefficient of 0.6 ($k < 1$) (Table 1). The enrichment of the grain boundary with Ti leads to the formation of Ni-Ti (Table 2) melting point depressant intermetallic particle. Ti has been discovered as one of the melting point depressant in Ni superalloy (Ernst et al, 1989). Thus, the presence of these Ti-rich particles at the grain boundary will enhance the stability of the liquid film resulting from the constitution liquation of γ' and MC carbide and consequently their penetration and wetting of the grain boundary which resulted in the revealed grain boundary microcracking (Fig. 6). The discussion above shows that grain boundary microfissuring cannot be considered in isolation due to constitutional liquation of γ' precipitates alone.

3.5. Microhardness and volume fraction studies

Figures 7a-c show the response of the alloy's hardness and primary γ' volume fraction to cooling from the weld simulated temperatures. It is generally believed that as cooling rate increases, there is a corresponding increase in hardness (Wusatowska-Sarnek et al, 2003). A high cooling rate results in a large degree of undercooling and increased supersaturation. This in return suppresses early precipitation during cooling and generates a large amount of nucleation sites and small size γ' (tertiary) with a small interparticle distance after cooling (Groh, 1996). Although it has been already stated in the present report that water quenching was chosen in order to preserve, as much as possible, the microstructural changes that occurred at the simulation temperatures. The observed variations in the hardness profile (Fig. 8) may be due to the temperature gradient from the weld line through the TMAZ. This temperature gradient during cooling may result in different re-precipitation responses of γ' precipitates in this region. The peak in hardness observed at 0.3 mm from weld line was due to the rapid nucleation and precipitation of tertiary γ' (Fig. 9a).

Table 1 Element partition coefficients in nickel based superalloy.

Element	Experimental k (Zhou et al, 1992)
Al	1.2
Co	1.1
Cr	1.05
Ni	1.05
Zr	0.06
Nb	0.4
Ti	0.6
Ta	0.7
Mo	0.85
W	1.4
Element	**Theoretical k (Taha and Kurz, 1981)**
B	0.0082
S	0.01
C	0.3

Table 2. Composition of the Ni-Ti intermetallic compound.

Element	Weight %	Atomic %
Ti	84.72	92.08
Cr	1.65	1.66
Ni	3.85	3.41
Hf	9.78	2.85

Constitutional liquation of primary γ' precipitates could also have been responsible for the trough in the hardness profile between 0.3 mm and 1 mm (Fig. 9c) in addition to the depletion of secondary γ' as reported by Preuss et al (2002) and also confirmed in the present work. The precipitation of the secondary γ' particles during cooling could be responsible for the next phase of increase in hardness from 1mm to approximately 2 mm from the bond line (Figs. 9 d-g). Further slow cooling from this region could result to the coarsening of secondary γ' until the distribution gives similar response to that of the base alloy (Fig. 9h). Figures 7a-b illustrate that the samples cooled from a simulation temperature of 1200°C give a similar response to the as-received IFW sample. This corroborates the report by Wang et al (2005) on the energy input based finite element process modeling of inertia welding (Fig. 10).

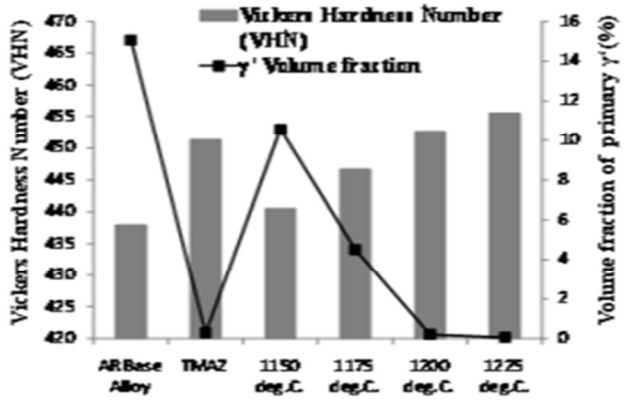

(a)

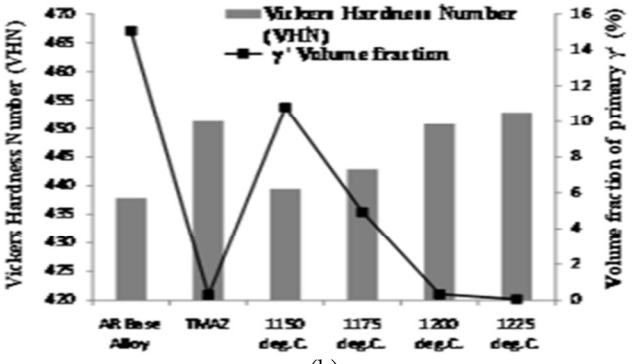

(b)

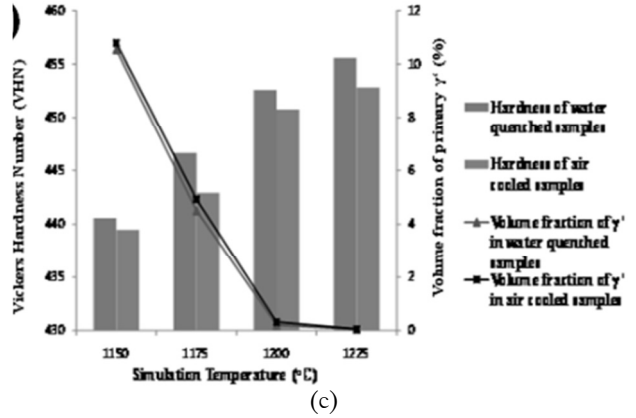

(c)

Fig.7. (a) Comparison of the hardness and primary γ' volume fraction of the base material and TMAZ with (a) water quenched samples(b) air cooled samples (c)The response of hardness and GB γ' particles to cooling rates from peak temperature in the simulated TMAZ.

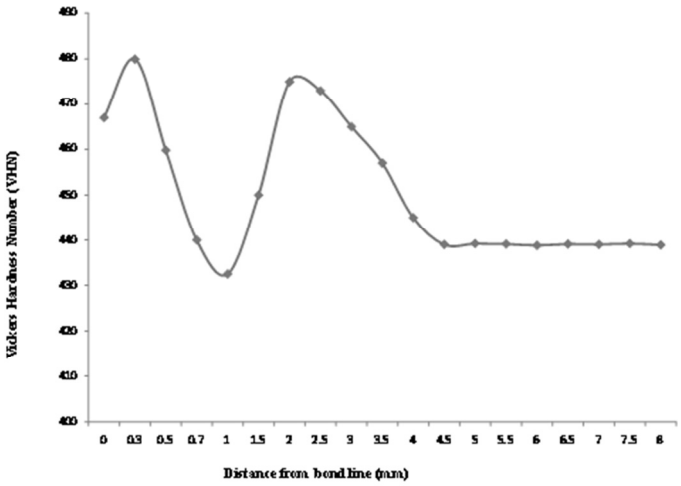

Fig.8. Response of the as received IFW RR1000 alloy's hardness to distance from the bond line

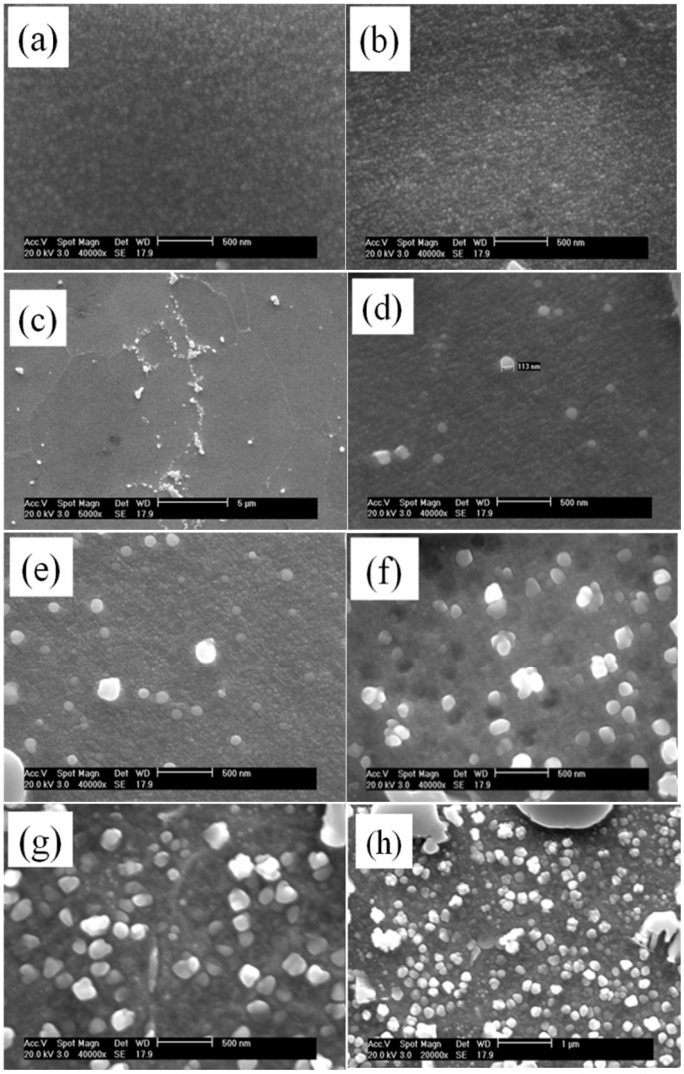

Fig. 9: SEM images of secondary and tertiary γ' of the IFW sample (a) at the bond line (b) 0.3 mm (c) 0.5 mm (d)1 mm (e) 1.5 mm (f) 1.7 mm (g) 2 mm and (h) 4 mm from the bond line.

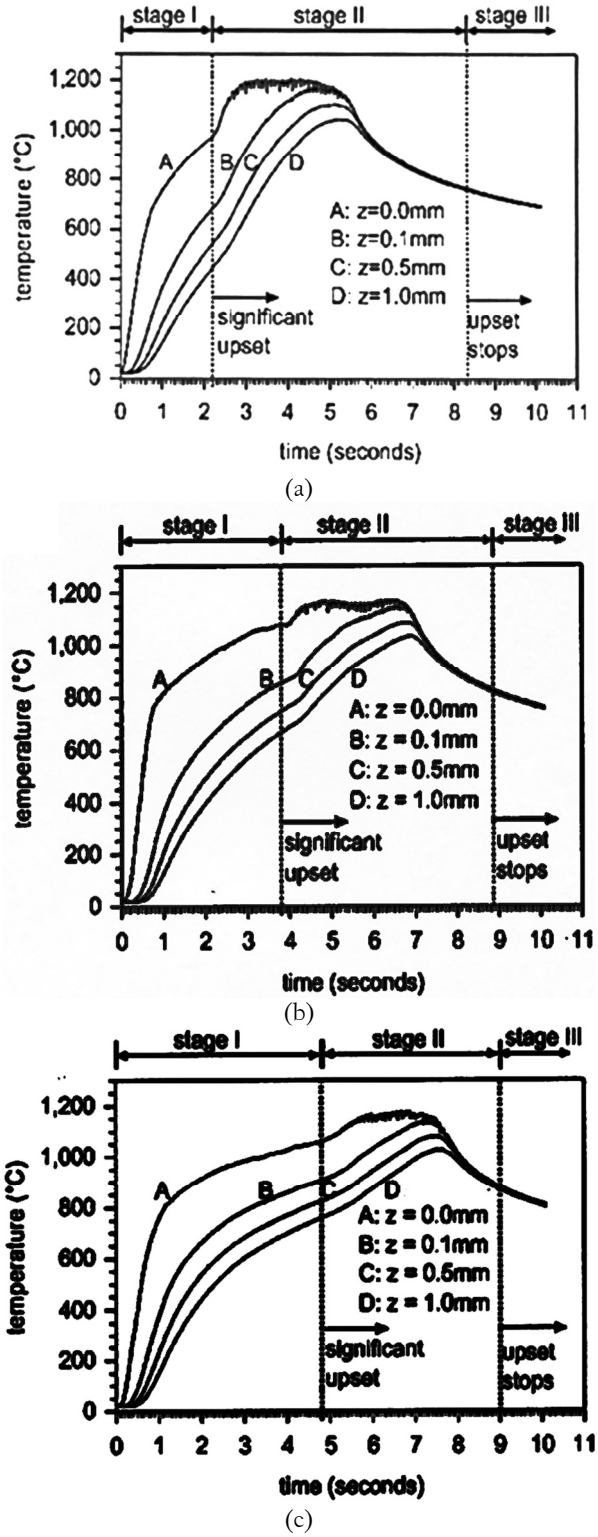

Fig. 10. The simulated thermal history of (a) low inertia, high initial rpm (b) medium inertia, medium initial rpm (c) high inertia, low initial rpm from the weld line. (Wang et al, 2005)

4. Conclusions

1. Re-solidified constituents were observed along cracked grain boundaries in the TMAZ of inertia friction welded RR1000 alloy and it is concluded that one of the factors responsible for TMAZ cracking in this alloy was grain boundary liquation.
2. Constitutional liquation of both intragranular and intergranular γ' precipitates was found to be contributing significantly to the TMAZ liquation.
3. Constitutional liquation of Ti-rich MC carbide precipitates was also found to contribute to the TMAZ liquation
4. Liquid films from liquated particles were observed to exhibit extensive penetration and wetting of grain boundaries even to the lower temperature subsolidus region of the TMAZ.
5. The results of the present study confirmed previous reports which indicated that rapid re-precipitation of γ' precipitates during solidification from weld temperature could contribute to TMAZ.
6. It is suggested that higher concentration of γ' forming elements in nickel base superalloys could promote constitutional liquation tendency of γ' particles by reducing the minimum required heating rate for particles of a given size to liquate, and by reducing the maximum γ' particle size that can withstand a particular heating rate without liquating.

Acknowledgements

The authors would like to appreciate Rolls Royce Plc for providing specimens and technical information.

References

Aksay, I.A.; Hoge, C.E. and Pask, J.A. 'Wetting under chemical-equilibrium and nonequilibrium conditions', J Phys Chem. 78:1178-1183, 1974.

Bjorneklett,; B.I.; Grong, O., Myhr, O.R. and Kluken, O.A. 'Additivity and isokinetic behaviour in relation to particle dissolution', Acta Mater. 46:6257, 1998.

Ernst, S.C.; Baeslack, W.A., Lippold J.C. 'Weldability of high-strength low-expansion Superalloys' Weld J. 68: 145, 1989.

Groh, J.R., 'Effect of cooling rate from solution heat treatment on waspaloy microstructure and properties', Superalloys', 621-626, 1996.

Jahnke, B. 'High-temperature electron beam welding of the nickel- base superalloy IN-738LC', Weld. J. 61: 343s–347s, 1982.

Koul, A.K.; and Wallace W. 'Note on the microstructural dependence of creep strength in inconel 700', Metallurgical and Materials Transactions A. 3A: 673- 675, 1982.

Lim, L.C.; Yi, J.Z., Liu, N. and Ma, Q. 'Mechanism of post-weld heat treatment cracking in Rene 80 nickel based superalloy', Mater. Sci. Technol. 18 (4): 407- 412, 2002.

Nakkalil, R.; Richards, N.L. and Chaturvedi, M.C. 'Influence of solidification mode on heat affected zone microfissuring in a nickel-iron base superalloy', Scripta Metall. Mater. 26: 1599–1603, 1992.

Ojo, O.A.; Richards, N.L. and Chaturvedi, M.C. 'Liquation of various phases in HAZ during welding of cast Inconel* 738LC', Mater. Sci. Technol. 20:1027–1034, 2004.

Ojo, O.A.; Richards, N.L. and Chaturvedi, M. C. 'Contribution of constitutional liquation of gamma prime precipitate to weld HAZ cracking of cast Inconel 738 superalloy', Scripta Mater. 50: 641, 2004.

Owczarski, W.A.; Duvall, D.S. and Sullivan, C.P. 'Model for heat-affected zone cracking in nickel-base superalloys', Weld. J. 45: 145s–155s, 1966.

Pepe, J.J.; and Savage, W.F. 'Effects of constitutional liquation in 18-Ni maraging steel weldments', Weld J. 46: 411s–422s, 1967.

Prager, M.; and Sines, G. 'Welding of precipitation-hardening nickel-base alloys', Weld. Res. Counc. Bull. No. 150:24–32, 1970.

Preuss, M.; Pang, J.W.L., Withers, P.J. and Baxter, G.J. 'Inertia welding nickel-based superalloy: Part I. Residual stress characterization', Metallurgical and Materials Transactions A: Physical Metallurgy and Materials Science, 33(10): 3215-3225, 2002.

Radhakrishnan, B. and Thompson, R.G. 'Phase diagram approach to study liquation cracking in alloy 718', Metall Trans;22A:887-902, 1991.

Radhakrishnan, B. and Thompson, R.G. 'The effect of weld heat-affected zone (HAZ) liquation kinetics on the hot cracking susceptibility of alloy-718', Metall. Trans. A, 24A:1409–15, 1993.

Reiso, O.; Ryum, N. and Strid, J. 'Melting of secondary-phase particles in Al-Mg-Si alloys', Metall Trans; 24A:2629-2641, 1993.

Romig, A.D. Jr.; Lippold, J.C. and Cieslak, M.J. 'Analytical electron microscope investigation of the phase transformations in a simulated heat-affected zone in alloy 800', Metall Trans;19A:35, 1988.

Sidhu, R.K.; Richards, N.L. and Chaturvedi, M.C. 'Effect of aluminium concentration in
filler alloys on HAZ cracking in TIG welded cast lnconel 738LC superalloy', Mater. Sci. Technol. 21 (10): 1119–31, 2005.

Sidhu, R.K.; Richards, N.L. and Chaturvedi, M.C. 'Post-weld heat treatment cracking inautogenous GTA welded cast Inconel 738LC superalloy', Mater. Sci. Technol. 23 (2): 203–13, 2007.

Silva, J.M. and A. Sousa E Brito. 'Microstructural evaluation of a new generation PM nickel base superalloy', Proceedings of the10th Portuguese Conference on Fracture, pp.1-6, 2006.

Soucail, M. and Bienvenu, Y. 'Dissolution of the γ′ phase in a nickel base superalloy at equilibrium and under rapid heating', Mater Sci Eng A. 220: 215, 1996.

Taha, M.; and Kurz, W. 'About microsegregation of nickel base superalloys'. Z. Metallkd. 72: 546-549, 1981.

Thamburaj, R.; Wallace, W. and Goldak, J.A. 'Post-weld heat-treatment cracking in Superalloys', Int. Met. Rev., 28 (1):1–22, 1983.

Wang L.; Preuss, M., Withers, P.J. Baxter, G. and Wilson, P. 'Energy-input-based finite-element process modelling of inertia welding', Metallurgical and Materials Transactions B: Process Metallurgy and Materials Processing Science, 36(4): 513-523, 2005.

Wusatowska-Sarnek, A.M.; Blackburn, M.J. and Aindow, M. 'Gamma Precipitation kinetics in P/M IN100 Thermec'2003, Pts 1-5,. 426-4: 767-772, 2003.

Zhou, J.; Wang, H. P., Doherty, R. and Perry, E. M. 'Solidification behavior and microstructure formation in a cast nickel based superalloy-experiment and modelling', in Proceedings of Superalloys Conference edited by S. D.Antolovich, R. W. Stusrud, R. A. Mackay, D. L. Anton, T. Khan, R. D. Kissinger and D. L. Klarstrom (The Minerals, Metals & Materials Society, 1992) p.165, 1992.